

Polymer Chemistry

Accepted Manuscript



This is an *Accepted Manuscript*, which has been through the Royal Society of Chemistry peer review process and has been accepted for publication.

Accepted Manuscripts are published online shortly after acceptance, before technical editing, formatting and proof reading. Using this free service, authors can make their results available to the community, in citable form, before we publish the edited article. We will replace this *Accepted Manuscript* with the edited and formatted *Advance Article* as soon as it is available.

You can find more information about *Accepted Manuscripts* in the [Information for Authors](#).

Please note that technical editing may introduce minor changes to the text and/or graphics, which may alter content. The journal's standard [Terms & Conditions](#) and the [Ethical guidelines](#) still apply. In no event shall the Royal Society of Chemistry be held responsible for any errors or omissions in this *Accepted Manuscript* or any consequences arising from the use of any information it contains.

Rapid Synthesis of Ultrahigh Molecular Weight and Low Polydispersity Polystyrene Diblock Copolymers by RAFT-mediated Emulsion Polymerization

Nghia P. Truong,^a Marion V. Dussert,^a Michael R. Whittaker,^a John F. Quinn^{*a} and Thomas P. Davis^{*a,b}

^a*ARC Centre of Excellence in Convergent Bio-Nano Science & Technology, Monash Institute of Pharmaceutical Sciences, Monash University, Parkville, Melbourne, Victoria 3052, Australia.*

^b*Department of Chemistry, University of Warwick, Coventry CV4 7AL, United Kingdom.*

Abstract

Reversible-deactivation radical polymerization techniques can be used to produce large and complex macromolecules for a wide range of applications. However, RAFT and related techniques are not readily applicable to the synthesis of well-defined, ultrahigh molecular weight polymers from monomers that have a low propagation rate coefficient (such as styrene). Herein we report the use of a novel water-soluble macro-stabilizer in the RAFT-mediated emulsion polymerization of styrene yielding an ultrafast synthesis of ultrahigh molecular weight, low polydispersity polystyrene diblock copolymers to very high conversion. This environmentally friendly emulsion technique produces uniform nanoparticles with precise control over molecular weight and particle size, presenting great potential for many applications.

Introduction

Over the last twenty years, the advent of reversible-deactivation radical polymerization (RDRP) techniques has revolutionized the field of precision polymer synthesis, providing powerful methods to prepare well-defined macromolecules with predetermined molecular weight, low polydispersity (PDI), and precisely defined end groups.¹⁻³ RDRP techniques such as atom-transfer radical polymerization (ATRP),⁴ nitroxide-mediated polymerization (NMP),⁵ and reversible addition fragmentation chain transfer polymerisation (RAFT)⁶ have been used to produce complex polymeric architectures for a wide range of applications. Importantly, these RDRP techniques can be carried out under environmentally friendly conditions, and so align with the global drive toward sustainable manufacturing.^{7,8} That said, RDRP techniques still fall well short of producing large, well-defined macromolecules with the same size and degree of precision as nature (such as, proteins, nucleic acids, etc.).⁹

To date, the routine synthesis of well-defined polymers with ultrahigh molecular weight (UHMW, number average molecular weight (M_n) $\geq 5 \times 10^5$ g mol⁻¹) using RDRP remains elusive.¹⁰ There are a number of limited examples in which UHMW polymers have been achieved. For example, Percec *et al.* reported the controlled synthesis of poly(methyl acrylate) with $M_n \sim 1 \times 10^6$ g mol⁻¹ mediated by Cu(0)-Me₆TREN catalysis in DMSO at 25 °C.¹¹ Poly(butyl methacrylate) with similar M_n was produced by miniemulsion polymerization using a copper-catalysed system with a redox initiator.¹² Functional UHMW polymers such as poly(2-hydroxyethyl methacrylate) and poly(2-(dimethylamino)ethyl methacrylate) have been synthesized using copper-catalysed RDRP.^{13,14} RAFT polymerization has also been used to produce UHMW poly(methyl methacrylate) and polyacrylamide with well-defined properties.^{10,15} In all these examples, monomers with high propagation rate coefficient (k_p) such as acrylates, acrylamides, and methacrylates were chosen. To our knowledge, there are no reports where in RDRP techniques have been successfully applied to synthesize well-defined UHMW polymers from monomers having low k_p (i.e., styrene).

Previous attempts to produce well-defined UHMW polystyrene (PSTY) have typically resulted in high polydispersity index (PDI) or poor control. Although UHMW polystyrenes can be synthesized in a microwave reactor (i.e., free radical polymerization) or by bulk polymerization using a rare earth-magnesium alkyl catalyst system, molecular weight distributions obtained tend to be very broad (i.e., $PDI > 2.1$).¹⁶⁻¹⁹ While using the RAFT technique enables polystyrenes with $PDI < 1.4$ to be produced, the highest reported M_n for narrow molecular weight distribution (MWD) polystyrene synthesized by this technique is $3.3 \times 10^5 \text{ g mol}^{-1}$.^{20,21} This is considerably lower than the M_n that can be attained using high- k_p monomers. Moreover, increasing the M_n of polystyrene to 10^6 g mol^{-1} leads to significant broadening of the MWD ($PDI = 2.3$).²¹ The key challenge in the synthesis of well-defined UHMW homopolymers or copolymers from styrene by RDRP stems from the interplay between polymerization rate and side reactions such as bimolecular termination and chain transfer to monomer (CTM). To produce UHMW polystyrene, a high polymerization rate for the polymer chains (e.g., at high temperature and/or high pressure) is needed: this often correlates with an increase in terminated chains.^{22,23} For instance, the value of monomer chain transfer constant, C_M (equal-to-the ratio of CTM and propagation rate coefficients, k_{tr}/k_p) is increased at high polymerization temperature resulting in very broad MWD of PSTY ($PDI > 2$) because CTM generally has higher activation energy than propagation.^{16,24} In addition, the increase in maximum attainable molecular weight of PSTY with pressure due to the reduced bimolecular coupling reaction at high pressure is not continuous but reaches a limiting value when C_M is high and CTM becomes dominant.²⁵ Therefore, synthesis strategies that increase the polymerization rate and also minimise side reactions are of the utmost importance for the synthesis of well-defined UHMW polystyrene.

One synthesis technique that exhibits both high polymerization rates and reduced side reactions is emulsion polymerization.^{26,27} This technique offers a number of other advantages over bulk or solution polymerization in that it is applicable to a broad range of monomers, provides excellent heat transfer, and is environmentally friendly.²⁸ In addition, emulsion polymerization is a versatile

tool for the synthesis of colloidal nanoparticles, which are of interest in areas such as surface coatings, sensor technology, catalysis, and nanomedicine.²⁹⁻³¹ The combination of emulsion polymerization and the RAFT chemistry has been successfully used to control the polymerization of styrene and produced well-defined homo- and diblock polystyrene with complex architectures and morphologies.³²⁻³⁴ However, to our knowledge, UHMW polystyrene with narrow MWD (i.e., PDI < 1.4) has not been successfully synthesized by emulsion polymerization or, for that matter, by any RDRP techniques.

Herein, we report the use of novel macromolecular chain transfer agents (macro-CTAs) in RAFT-mediated emulsion polymerization to synthesize UHMW diblock polystyrenes with M_n up to 10^6 g mol⁻¹ and PDI < 1.4. The novel macro-CTAs based on N-Hydroxyethyl acrylamide (HEAA) and Poly(ethylene glycol) methyl ether acrylate (PEGA) were synthesized by judiciously selecting the components and polymerization conditions. Polymerization kinetics of emulsion polymerizations using the novel macro-CTAs was then studied. Further, the excellent stabilizing characteristic provided a facile method to control both molecular weight and particle size of the final latex with a linear relationship established between molecular weight and particle size.

Experimental Section

Materials

Ethanol (97%), carbon disulfide (>99.9%), p-Toluenesulfonyl chloride (>99%), and dimethyl sulfoxide (>99.9%, anhydrous) were purchased from Sigma-Aldrich and used as received. Potassium hydroxide (pellet, AR grade) was obtained from ChemSupply and used as received. Poly(ethylene glycol) methyl ether acrylate average $M_n \sim 480$ (PEGA, Sigma-Aldrich), N-hydroxyethyl acrylamide (HEAA, 97%, Sigma-Aldrich) and styrene (>99%, Sigma-Aldrich) were passed through a column of basic alumina (activity I) to remove inhibitor prior to use. 4,4'-Azobis(4-cyanopentanoic acid) (ACPA, 98%, Alfa Aesar) was recrystallized twice in methanol

prior to use. MilliQ water (resistivity $> 18.2 \text{ M}\Omega\text{cm}^{-1}$) was generated using a Millipore MilliQ Academic Water Purification System. All other chemicals and solvents used were of at least analytical grade and used as received.

Synthesis of chain transfer agent (CTA), 4-cyano-4-(ethylthiocarbonothioylthio)pentanoic acid (ECT). The synthesis of ECT was carried out by modifying literature procedures.^{35,36} KOH aqueous solution (50%; 6.72 g, 0.12 mol) was added dropwise over 5 min at 0 °C under nitrogen atmosphere, to a stirred solution of ethanethiol (7.4 mL, 0.10 mol) in water/acetone (20/5; 25 mL). Carbon disulfide (7.61 g, 0.10 mol) was added in one portion. The solution was stirred at 24 °C for 30 min, and cooled to -5 °C in an ice-acetone bath. P-toluenesulfonyl chloride (9.91 g, 0.052 mol) was added in aliquots over 5 min and the resulting solution was stirred at 24 °C for another hour. The mixture was then stirred at 45 °C for 30 min followed by dissolution in DCM (150 mL). After washing with water twice ($2 \times 50 \text{ mL}$), the organic layer was separated and volatiles evaporated under a stream of purity air yielding the orange crude product. This crude product was used for next step without purification. The crude product (6.0 g, 0.022 mol) and 4,4'-azobis(4-cyanovaleic acid) (9.2 g, 0.032 mol) were dissolved in degassed ethyl acetate (300 mL). The mixture was refluxed for 24 h under nitrogen, cooled to 25 °C, and the solvent was removed under a stream of purity air. The residue was purified by column chromatography on silica gel using a gradient solvent mixture of petroleum benzine : ethyl acetate (3: 2 slowly changed to 1 : 2) to yield the product as a yellow oil. After complete removal of the solvents, an orange solid was formed (8.1 g, 70% yield). ^1H NMR (CDCl_3) ppm: 3.32 (q, $J = 7.5 \text{ Hz}$, 2H, $\text{CH}_3\text{-CH}_2\text{-}$), 2.56 - 2.34 (m, 4H, $\text{-CH}_2\text{-CH}_2\text{-}$), 1.86 (s, 3H, -C-CH_3), 1.34 (t, $J = 7.5 \text{ Hz}$, 2H, $\text{CH}_3\text{-CH}_2\text{-}$). ^{13}C NMR (CDCl_3) ppm: 171.6, 119.0, 46.3, 33.6, 31.5, 29.7, 24.5, 12.9.

Synthesis of macro-chain transfer agents (macro-CTAs), $P(\text{PEGA-co-HEAA})\text{-SC(=S)SC}_2\text{H}_5$. All polymerizations were carried out in 25 mL vials equipped with a magnetic stirrer. Four macro-CTAs with different chain lengths were synthesized by varying the ratios of monomers, CTA, and initiator. A typical polymerization to synthesize macro-CTA (A3) was as follows: PEGA (3.34 g,

6.96×10^{-3} mol), HEAA (1.00 g, 8.70×10^{-3} mol), ECT (57 mg, 2.17×10^{-4} mol), and ACPA (3 mg, 1.09×10^{-5} mol) were dissolved in DMSO (12 mL, anhydrous). The vial was sealed with a rubber septum and the solution deoxygenated by sparging with nitrogen for 60 min. After polymerizing for 7 h at 60 °C, the reaction was cooled to 0 °C by an ice bath and exposed to air. A 50 μ L aliquot of the solution was sampled to determine conversion by ^1H NMR. The solution was then dialyzed against acetone (200 mL) for 1 h to remove DMSO using dialysis membrane with molecular weight cut-off 3.5 kDa. The polymer was recovered by precipitating into a large excess of diethyl ether (200 mL), isolating the precipitated polymer by centrifugation, and redissolving it in acetone. This purification process was repeated three times. The product was dried under high vacuum for 48 h to give a yellow sticky solid (1.61 g, yield 59%).

RAFT-mediated emulsion polymerization of styrene in water at 80 °C using P(PEGA-co-HEAA)-SC(=S)SC₂H₅ as macro-CTA. All emulsion polymerizations were carried out in 25 mL vials equipped with a magnetic stirrer. Different chain lengths of polystyrene blocks were synthesized by changing the ratio of styrene to macro-CTA. A typical polymerization was as follows: ACPA (2.0 mg, 7.0×10^{-6} mol) was dissolved in MilliQ water (20 mL) by stirring for 30 min. 4 mL of the ACPA solution (3.5×10^{-4} mol L⁻¹) was used to dissolve macro-CTA A3 (70 mg, 5.5×10^{-6} mol) in a 25-mL vial. The vial was sealed with a rubber septum and the solution was deoxygenated by sparging with nitrogen for 25 min. Simultaneously, styrene (0.5 mL) was added into 1.5-mL vial and also sparged with nitrogen for 25 min. After 25 min, a portion of the deoxygenated styrene (0.4 mL, 3.5×10^{-3} mol) was added into the 25 mL vial using a gas-tight syringe and the emulsion was sparged with nitrogen for a further 5 min. After a total nitrogen sparging time of 30 min, the emulsion was placed in an oil bath at 80 °C. After 6 h stirring at 80 °C and 300 rpm, the emulsion polymerization was stopped by cooling to 0 °C in an ice bath and exposing to air. For the kinetic study, approximately 0.1 mL of the emulsion was sampled periodically during the polymerization using a gas-tight syringe. These samples were used to evaluate conversion (by ^1H NMR), molecular weight (by SEC) and particle size (by DLS) as a function of reaction time.

Characterization Techniques

¹H Nuclear Magnetic Resonance (NMR). All NMR spectra were recorded on a Bruker Advance III 400 MHz spectrometer using an external lock and referenced to the residual nondeuterated solvent. A mixture of deuterated acetone and deuterated chloroform (ratio 10 to 1) was used in the analysis of conversion of the emulsion polymerizations by ¹H NMR.

Size Exclusion Chromatography (SEC). SEC analyses of polymer samples were performed using a Shimadzu modular system comprising a DGU-12A degasser, an SIL-20AD automatic injector, a 5.0 μm bead-size guard column (50 × 7.8 mm) followed by three KF-805L columns (300 × 8 mm, bead size: 10 μm, pore size maximum: 5000 Å), a SPD-20A ultraviolet detector, and an RID-10A differential refractive-index detector. The temperature of columns was maintained at 40 °C using a CTO-20A oven. The eluent was N,N-dimethylacetamide (HPLC grade, with 0.03% w/v LiBr) and the flow rate was kept at 1 mL/min using a LC-20AD pump. A molecular weight calibration curve was produced using commercial narrow molecular weight distribution polystyrene standards with molecular weights ranging from 500 to 2 × 10⁶ g mol⁻¹. Polymer solutions at approx. 2 mg mL⁻¹ were prepared and filtered through 0.45 μm filters prior to injection.

Dynamic Light Scattering (DLS). Dynamic light scattering measurements were performed using a Malvern Zetasizer Nano Series running DTS software and operating a 4 mW He-Ne laser at 633 nm. Analysis was performed at an angle of 173° and a constant temperature of 25 °C. The sample refractive index (RI) was set at 1.59 for polystyrene. The dispersant viscosity and RI were set to 0.89 Ns.m⁻² and 1.33, respectively. The number-average hydrodynamic particle size and polydispersity index are reported. The polydispersity index (PSD) was used to describe the width of the particle size distribution. It was calculated from a Cumulants analysis of the DLS measured intensity autocorrelation function and is related to the standard deviation of the hypothetical Gaussian distribution (i.e., $PSD = \sigma^2/Z_D^2$, where σ is the standard deviation and Z_D is the Z average mean size). A typical sample preparation for DLS measurement is as follows: a drop (about 20 μL) of hot emulsion latex was added into 1 mL of filtered MilliQ water in a cuvette. The cuvette was

shaken and placed in the DLS instrument. All samples were incubated in the DLS instrument for 5 min at 25 °C prior to measurement.

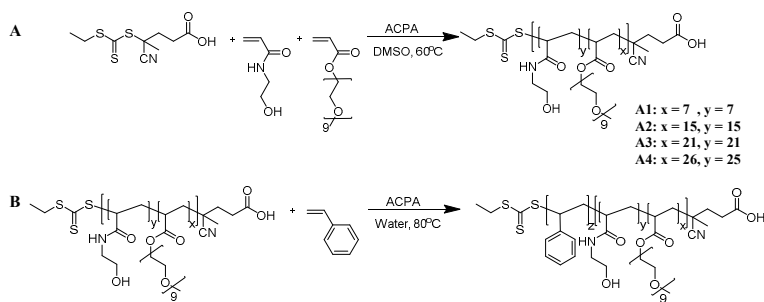
Transmission Electron Microscopy (TEM). TEM images were recorded without staining using Tecnai F20 transmission electron microscope at an accelerating voltage of 200 kV at ambient temperature. A typical TEM grid preparation was as follow: 5 μ L aliquot of a 0.1 wt% solution was dropped on a Formvar-film copper grid (GSCu100F-50, Proscitech), after which samples were allowed to dry under air.

UV-Vis spectrophotometry. UV-Vis absorption spectra were recorded at ambient temperature on a Shimadzu UV-3600 spectrophotometer. The product of reaction 4 was freeze-dried and redissolved in THF for measurement using a quartz cuvette.

Results and Discussion

Synthesis of macro-CTAs. As a precursor to the emulsion polymerization of styrene, a series of novel electrosteric stabilizers / macro-CTAs was first synthesized by RAFT-mediated solution polymerization. Specifically, P(PEGA-co-HEAA)-SC(=S)SC₂H₅ with four different molecular weights (A1-A4, see Scheme 1.A) was prepared by polymerizing PEGA and HEAA in anhydrous DMSO for 7 h at 60 °C. ECT was used as the CTA in this work due to its high stability in water and its suitability for controlling the polymerization of a wide range of monomers, including acrylates, acrylamides and styrenics.^{37,38} PEGA and HEAA were chosen as macro-CTA components for a number of reasons. Specifically, PEGA confers excellent antifouling characteristics; while the highly hydrophilic HEAA improves the water solubility of the resulting macro-CTAs and reduces partitioning of the macro-stabilizers within the styrene droplets and/or on water/droplet interfaces.³⁹⁻⁴² Further, polymers synthesized from PEGA and HEAA are biocompatible presenting the potential use of the formed nanoparticles for biomedical applications.⁴³⁻⁴⁶ The molar ratio of HEAA to PEGA in all macro-CTAs was kept constant at 1 to 1, as calculated from conversions and confirmed by the representative ¹H NMR of the macro-CTA A2 (Figure S1.A). P(PEGA)-SC(=S)SC₂H₅ and P(HEAA)-SC(=S)SC₂H₅ homopolymers could not be used as macrostabilizer due to their inability

to effectively stabilize the emulsion formed (data not shown). By varying the monomer to CTA and initiator molar ratios, different degrees of polymerization of HEAA and PEGA were obtained (ranging from 5 to 25). This suite of different chain length macro-stabilizers was used to study the influence of chain length on the stability of the emulsion polymerizations and the possibility of transforming morphology during polymerization (see Table 1). The difference between the M_n values of the macro-CTAs obtained using SEC and those expected from the monomer to CTA feed ratio could be ascribed to differences in the hydrodynamic volume of the polystyrene standards used for SEC calibration and that of the macro-CTAs.⁴⁷ High chain-end fidelity of each macro-CTA is a crucial factor for ensuring quantitative block formation during the emulsion polymerizations.⁴⁸ As such, ACPA was chosen as the initiator in this first step because the initiating radical generated is identical to the leaving group of the CTA, thus ensuring that all of the macro-stabilizers have the same end group. Further, optimized conditions such as low relative concentrations of initiator (i.e., 5% or 8% of [CTA]), short polymerization time (i.e., 6 h), and low temperature (i.e., 60 °C) were carefully selected to yield macro-CTAs with a relatively low PDI (< 1.22) and a theoretically low number fraction of dead chains (i.e., about 2%, calculated from [ECT] and consumed [ACPA] after 6h). Symmetrical and unimodal MWDs (as shown in Figure S1.B) further confirmed the low levels of termination and irreversible chain transfer during the polymerization. In short, four well-defined macro-CTAs with HEAA and PEGA repeat units were successfully synthesized by judiciously selecting the components and polymerization conditions.



Scheme 1. (A) Synthesis of P(PEGA-co-HEAA)-SC(=S)SC₂H₅ macro-CTAs. (B) RAFT-mediated emulsion polymerization of styrene.

Table 1. SEC and ^1H NMR data for P(PEGA-co-HEAA)-SC(=S)SC₂H₅ macro-CTAs with different molecular weight (A1-A4), prepared by RAFT polymerization of HEAA and PEGA at 60 °C in DMSO for 7 h using ACPA as initiator.

| Macro-CTA | [HEAA]:[PEGA]:[CTA]:[I] | SEC ^a | | ^1H NMR | | | | $M_{n,\text{theory}}^f$ (g/mol) |
|-----------|-------------------------|------------------|------|-------------------|-------------------|--------------------|-------------------|------------------------------------|
| | | M_n (g/mol) | PDI | Conversion (%) | | Repeating unit (n) | | |
| | | | | HEAA ^b | PEGA ^c | HEAA ^d | PEGA ^e | |
| A1 | 400:320:20:1 | 7,100 | 1.15 | 37 | 46 | 7 | 7 | 4,428 |
| A2 | 250:200:12:1 | 11,100 | 1.14 | 76 | 90 | 15 | 15 | 9,188 |
| A3 | 800:640:20:1 | 15,600 | 1.20 | 51 | 66 | 21 | 21 | 12,758 |
| A4 | 1000:800:20:1 | 20,600 | 1.22 | 50 | 65 | 25 | 26 | 15,618 |

^a SEC data measured in DMAc + 0.03 wt% of LiBr solution and using PSTY standards for calibration. ^b Conversion of HEAA was calculated by the integral area of a peak at 5.5 ppm ($I_{5.5}$) and peaks in the range 4.5-5.0 ($I_{4.5-5.0}$) using the following equation: Conversion of HEAA = $100 \times I_{5.5} / I_{4.5-5.0}$. ^c Conversion of PEGA was calculated by the integral area of a peak at 5.9 ppm ($I_{5.9}$) and peaks in the range 3.9-4.2 ($I_{3.9-4.2}$) using the following equation: Conversion of HEAA = $100 \times 2 \times I_{5.9} / I_{3.9-4.2}$. ^d Number of repeating units of HEAA was calculated using the following equation: $n = \text{conversion} \times [\text{HEAA}] / [\text{CTA}]$. ^e Number of repeating units of PEGA was calculated using the following equation: $n = \text{conversion} \times [\text{PEGA}] / [\text{CTA}]$. ^f $M_{n,\text{theory}}$ was calculated using the following equation: $M_{n,\text{theory}} = n_{\text{HEAA}} \times 115 + n_{\text{PEGA}} \times 480 + 263$.

Kinetic study of RAFT-mediated emulsion polymerizations. To understand the characteristics of the RAFT-mediated emulsion polymerization of styrene using P(PEGA-co-HEAA)-SC(=S)SC₂H₅ as stabilizers, kinetics were first studied using A3 as a model stabilizer. To commence the emulsion polymerization (see scheme 1.B), ACPA (0.4 mg, 1.4×10^{-6} mol) and A3 (70 mg, 5.5×10^{-6} mol) were first dissolved in MilliQ-water (4 mL) and then deoxygenated by sparging with nitrogen for 25 min. Styrene (~ 0.5 mL) was simultaneously deoxygenated in a separated vial, and after 25 min of purging with nitrogen, the deoxygenated styrene (0.4 mL, 3.5×10^{-3} mol) was transferred into the solution of initiator and macro-CTA using a gas-tight syringe. Deoxygenating the styrene in a separate vial and then transferring into the reaction vial ensured the precise amount of styrene at the

start of the polymerization, thereby ensuring reproducibility of the experiments. The emulsion polymerization was commenced after a further 5-min of sparging with nitrogen to ensure complete deoxygenation of the reaction mixture. Table 2 summarizes the polymerization kinetics and particle size data measured using ^1H NMR, SEC, and DLS. From these data, the RAFT-mediated emulsion polymerization of styrene using P(PEGA₂₁-co-HEAA₂₁)-SC(=S)SC₂H₅ as macro-CTA appears to follow a similar concept to other emulsion polymerization systems as previously reported by Hawkett *et al.*⁴⁹, and Charleux *et al.*⁵⁰ This concept, referred to as polymerization-induced self-assembly (PISA), can be classified into two stages. In the first (i.e., initiation) stage in the aqueous phase, sparingly dissolved styrene slowly added to the macro-CTA (i.e., ~ 2% over ~ 2 h) presumably by a typical addition-fragmentation process as expected in a solution polymerization mediated by RAFT (see Figure 1.A). Once the styrene block has sufficient hydrophobicity to form nanoparticles by self-assembly, the second stage commenced in the hydrophobic phase (i.e., inside the particle cores). During this second stage of polymerization, styrene copolymerised ultrafast with macro-CTA reaching 96% conversion after only 2 h and producing a diblock copolymer with M_n of $74 \times 10^3 \text{ g mol}^{-1}$ and a PDI value of 1.21. The accelerated rate of polymerization of styrene during the second stage can be explained by the compartmentalization or confined space effect of growing polymeric radicals.^{51,52} Figure 1.B shows excellent agreement between the M_n determined by SEC and that predicted from theory, and the linear increase in M_n with conversion, which are indicative of a well-controlled RDRP mechanism. In addition, low PDI as well as the unimodal and symmetrical MWDs shown in Figure 1.C confirms a low number of terminated chains even at very high conversion. These results also suggest little to no side reactions such as bimolecular coupling and CTM occurring during the emulsion polymerization due to the segregation or isolation of growing polymeric radicals.^{27,31} Importantly, the reduction of side reactions such as CTM may allow the synthesis of well-defined UHMW PSTY by emulsion polymerization because CTM is assumed to be the kinetic event responsible for the desorption of small radicals from the emulsion droplets and termination of the polymer chain propagation.^{26,27} Further, the number of particles per

litre (N_c) calculated using equation 1 was constant during the second stage of the polymerization (see Table 2).⁵³ This result indicates that the characteristics of emulsion polymerization controlled by P(PEGA₂₁-co-HEAA₂₁)-SC(=S)SC₂H₅ are similar to an ideal miniemulsion where the number of particles during the polymerization is unchanged (i.e., a one-to-one copy).^{22,27} Interestingly, the total number of macro-CTA chains stabilizing one nanoparticle (N_{MCTA} , calculated using equation 2) was around 2700. This is much larger than a typical aggregation number found for surfactants but very similar to the N_{MCTA} of poly(acrylic acid) macro-CTA.⁵³ These large N_{MCTA} values are consistent with the hypothesis that all macro-CTAs are localized on the surface of the particles during the polymerization, thus providing excellent stability to the emulsion and the product nanoparticles.⁵³ Examination of the TEM images in Figure 2 and DLS data in Table 2 showed that the nanoparticles were close to monodisperse (i.e., PSD < 0.1), with the particle sizes uniformly increasing during the second stage of the emulsion polymerization. It is worth noting that, without stirring and at low conversion, styrene monomer in the emulsion forms an organic phase which separates out above the water phase. This phase separation between styrene and water allows the characterization of hydrodynamic volume of the nanoparticles in the water phase by DLS even at low conversion. Altogether, these results confirm that P(PEGA₂₁-co-HEAA₂₁)-SC(=S)SC₂H₅ is an excellent stabilizer and macro-CTA for the emulsion polymerization of styrene due to the anti-fouling properties of the PEGA component together with the high hydrophilicity of HEAA component.

Equation 1:

$$N_c = \frac{\text{Conv } V_s d_s}{\frac{4}{3} \pi r_h^3 d_p V_w} (\text{L}^{-1})$$

where N_c is the number of particles per litre, Conv. is conversion of styrene, V_s is volume of styrene, d_s is density of styrene, r_h is hydrodynamic radius of particles measured by DLS, d_p is density of polystyrene, and V_w is volume of water.

Equation 2:
$$N_{MCTA} = \frac{mol_C N_A V_w}{N_c}$$

where N_{MCTA} is the number of macro-CTA per particles, mol_C is molarity of macro-CTA, N_A is Avogadro's number, and V_w is the volume of water.

Table 2. ^1H NMR, SEC, and DLS data for the RAFT-mediated emulsion polymerization of styrene (0.4 mL) in water (4 mL) at 80 °C using P(PEGA₂₁-co-HEAA₂₁)-SC(=S)SC₂H₅ (A3, 70 mg) as Macro-CTA and ACPA (0.4 mg) as an initiator.

| Time (min) | ^1H NMR | | SEC ^c | | DLS ^d | | N_c^e (L ⁻¹) | N_{MCTA}^f |
|------------|-----------------------------|---|---------------------------|------|------------------|-------|----------------------------|--------------|
| | Conversion ^a (%) | $M_{n,theory}^b$ (g mol ⁻¹) | Mn (g mol ⁻¹) | PDI | D_h (nm) | PSD | | |
| 90 | 2 | 14,085 | 15,600 | 1.19 | 15 | 0.367 | 10×10^{17} | 8500 |
| 195 | 24 | 28,680 | 29,700 | 1.24 | 52 | 0.050 | 3.0×10^{17} | 2700 |
| 210 | 60 | 52,563 | 48,000 | 1.23 | 69 | 0.055 | 3.0×10^{17} | 2700 |
| 225 | 81 | 66,495 | 63,000 | 1.21 | 74 | 0.082 | 3.0×10^{17} | 2700 |
| 240 | 96 | 76,446 | 74,000 | 1.21 | 78 | 0.048 | 3.0×10^{17} | 2700 |

^a Conversion of styrene was calculated by the integral area of a peak at 5.7 ppm ($I_{5.7}$) and a peak in the range 6.3-7.5 ($I_{6.3-7.5}$) using the following equation: Conversion of styrene = $100 \times 5 \times I_{5.7} / I_{6.3-7.5}$. ^b $M_{n,theory}$ was calculated using the following equation: $M_{n,theory} = \text{Conversion} \times 104 \times 638 / 100 + 12758$. ^c SEC data measured in DMAc + 0.03 wt% of LiBr solution and using PSTY standards for calibration. ^d Dynamic light scattering measurements were made at 25 °C and reported values are an average of 5 measurements. ^e Number of particles per litre (N_c) was calculated using the equation 1. ^f Number of macro-CTA per particles (N_{MCTA}) was calculated using the equation 2.

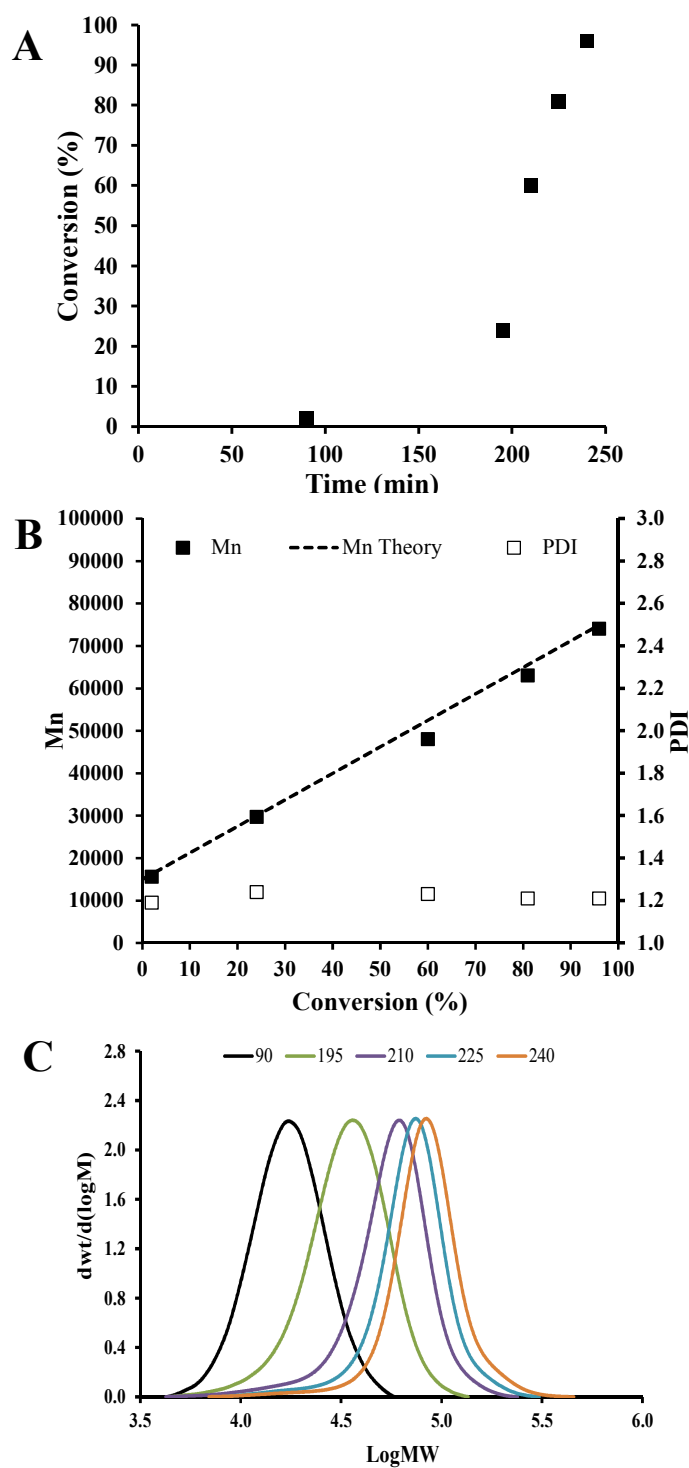


Figure 1. (A) Conversion vs time, (B) number average molecular weight and PDI vs conversion, and (C) molecular weight distributions for the RAFT-mediated emulsion polymerization of styrene in water at 80 °C using P(PEGA₂₁-co-HEAA₂₁)-SC(=S)SC₂H₅ (A3) as macro-CTA and ACPA as initiator.

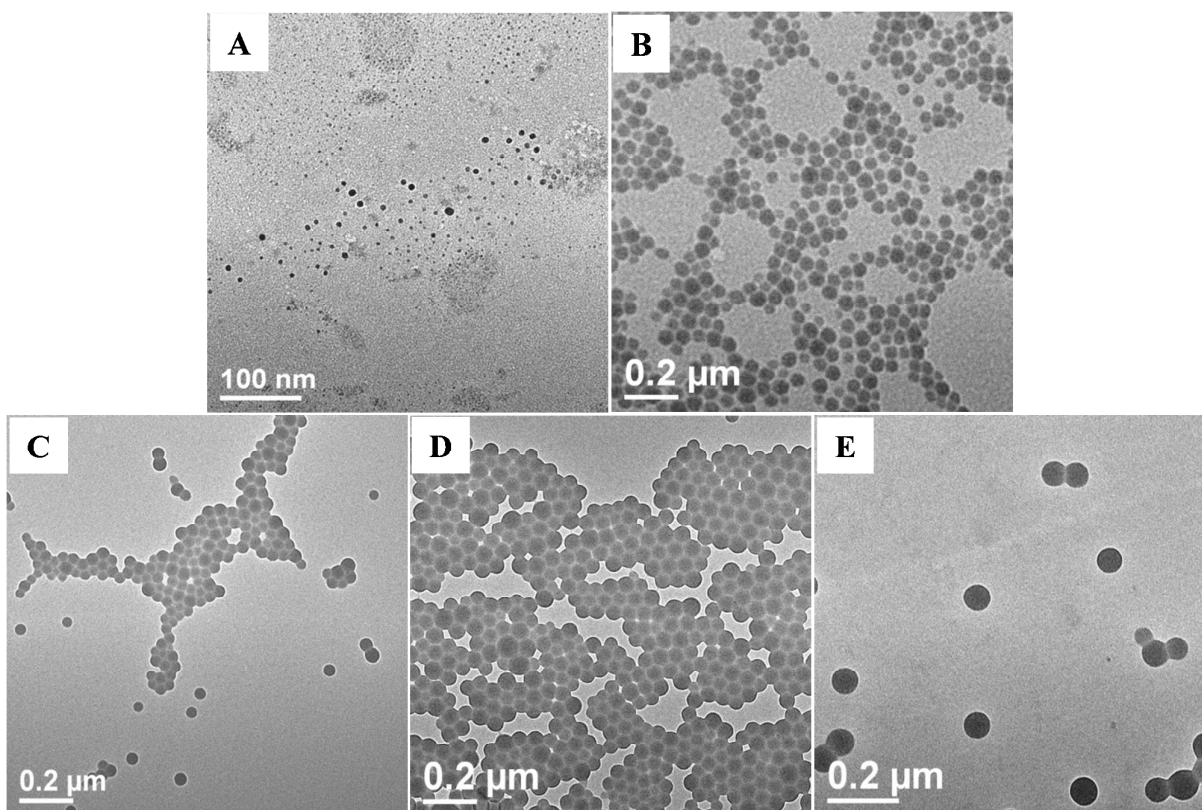


Figure 2. TEM images of the particles formed by RAFT-mediated emulsion polymerization of styrene in water using P(PEGA₂₁-co-HEAA₂₁)-SC(=S)SC₂H₅ (A3) as macro-CTA at different time points (A) 90 min, (B) 195 min, (C) 210 min, (D) 225 min, and (E) 240 min.

Synthesis of ultrahigh molecular weight and low PDI polystyrene diblock copolymer. After confirming that P(PEGA₂₁-co-HEAA₂₁)-SC(=S)SC₂H₅ was both an excellent stabilizer and suitable macro-CTA for RAFT-mediated emulsion polymerization of styrene with high polymerization rates and reduced side reactions, we aimed to synthesize UHMW polystyrene diblock copolymers using this same macro-CTA (A3). By appropriate variation of the styrene to macro-CTA ratio, P(PEGA₂₁-co-HEAA₂₁)-b-P(STY_z)-SC(=S)SC₂H₅ was synthesized with three different molecular weights (see Reactions 1-3 in Table 3). After 6 h polymerization time, all reactions reached very high conversions (> 90%). Reaction 2 shows that using our emulsion system it is possible to synthesize UHMW polystyrene diblock copolymer ($M_n \sim 5 \times 10^5 \text{ g mol}^{-1}$) with narrow molecular weight

distribution (PDI = 1.32). Further, the particle size distributions remained close to monodisperse throughout the polymerization (see Table 3 and Figure S2). However, when the ratio of styrene to A3 in reaction 3 was increased to double than that in Reaction 2 (i.e., to target a diblock copolymer with $M_n \sim 1 \times 10^6 \text{ g mol}^{-1}$), the PDI and PSD increased to 1.60 and 0.166, respectively. By comparing the MWD and the calculated N_{MCTA} of Reaction 1 and 2 to Reaction 3 (see Figure S3 and Table 3), we hypothesized that aggregation of nanoparticles during polymerization caused the increase in both PDI and PSD for Reaction 3 even though all reactions had the same solid content (i.e., 20%). To test this hypothesis, macro-CTA A4 with longer chain lengths (i.e., higher stabilizing capacity) was synthesized and subsequently employed in the emulsion polymerization of styrene. Data for Reaction 4 (see Table 3) showed that, with a similar N_{MCTA} to that found for Reaction 3, A4 could stabilize the emulsion polymerization of styrene. Moreover, the resulting polystyrene diblock copolymer was of ultrahigh molecular weight ($M_n \sim 1 \times 10^6 \text{ g mol}^{-1}$) and relatively low PDI (< 1.4). To our knowledge this is the first report of polystyrene diblock copolymer with such a high molecular weight and relatively narrow MWD. UV signals at 310 nm from the UV detector attached to the SEC (see Figure S4.A) and from the UV-vis spectrometer (see Figure S4.A) confirms the presence of the trithiocarbonate in the diblock copolymer. Importantly, the resulting polymer was characterized by a symmetrical and unimodal MWD (as shown in Figure 3.A) suggesting that the RDRP mechanism remained operative even to this very high conversion and molecular weight. In addition, the particle size distribution of the polystyrene diblock copolymer with $M_n \sim 1 \times 10^6 \text{ g mol}^{-1}$ and PDI < 1.4 was highly uniform (i.e., PSD ~ 0.015 , see Table 3 and Figure 3.B), which demonstrates the excellent electrosteric stabilization provided by the P(PEGA-co-HEAA)-SC(=S)SC₂H₅ macro-CTA. Overall, the strategy of applying emulsion polymerization to increase the polymerization rate and reduce side reactions was achieved using a novel anti-fouling, anti-aggregation macro-CTA (P(PEGA-co-HEAA)-SC(=S)SC₂H₅). By utilizing this novel emulsion system, UHMW and low PDI polystyrene diblock copolymer can be produced in the latex of nearly monodisperse nanoparticles.

Table 3. ¹H NMR, SEC, and DLS data for the RAFT-mediated emulsion polymerization of styrene in water at 80 °C for 6 h using ACPA as an initiator with different macro-CTAs. The solid content after polymerization was 20%.

| Rxn | Macro-CTA | [Styrene]:[Macro-CTA]:[I] | ¹ H NMR | | SEC ^c | | DLS ^d | | N_c^e (L ⁻¹) | N_{MCTA}^f |
|-----|-----------|---------------------------|-----------------------|---|------------------------------|------|------------------|-------|----------------------------|--------------|
| | | | Conc ^a (%) | $M_{n,theory}^b$ (g mol ⁻¹) | M_n (g mol ⁻¹) | PDI | D_h (nm) | PSD | | |
| 1 | A3 | 2,790:1:0.3 | 96 | 291,393 | 278,000 | 1.29 | 124 | 0.049 | 2.0×10^{17} | 2300 |
| 2 | A3 | 5,253:1:0.3 | 92 | 515,393 | 489,000 | 1.32 | 155 | 0.020 | 8.0×10^{17} | 2500 |
| 3 | A3 | 11,907:1:0.3 | 93 | 1,164,448 | 720,600 | 1.60 | 83 | 0.166 | 5.0×10^{17} | 1600 |
| 4 | A4 | 14,577:1:0.4 | 91 | 1,395,166 | 1,043,700 | 1.39 | 174 | 0.015 | 6.0×10^{16} | 1300 |
| 5 | A2 | 1286:1:0.3 | 96 | 137,614 | 95,000 | 1.30 | 144 | 0.025 | 1.0×10^{17} | 7700 |
| 6 | A1 | 1550:1:0.3 | 91 | 151,101 | 149,000 | 1.24 | 145 | 0.017 | 1.0×10^{17} | 7000 |

^a Conversion of styrene was calculated by the integral area of a peak at 5.7 ppm ($I_{5.7}$) and a peak in the range 6.3-7.5 ($I_{6.3-7.5}$) using the following equation: Conversion of styrene = $100 \times 5 \times I_{5.7} / I_{6.3-7.5}$. ^b $M_{n,theory}$ was calculated using the following equation: $M_{n,theory} = \text{Conversion} \times 104 \times [\text{Styrene}] / [\text{MCTA}] / 100 + M_{n,theory} \text{ of MCTA}$. ^c SEC data measured in DMAc + 0.03 wt% of LiBr solution and using PSTY standards for calibration. ^d Dynamic light scattering measurements were made at 25 °C and reported values are an average of 5 measurements. ^e Number of particles per litre (N_c) was calculated using the equation 1. ^f Number of Macro-CTA per particles (N_{MCTA}) was calculated using the equation 2.

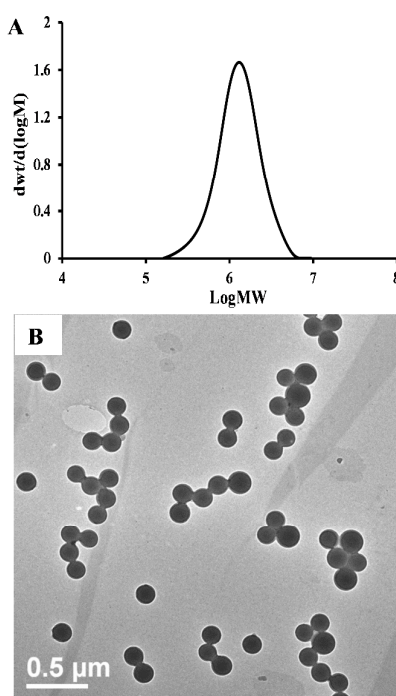


Figure 3. (A) Molecular weight distribution and (B) TEM images of the product polymer of RAFT-mediated emulsion polymerization of styrene in water at 80 °C for 6 h using P(PEGA₂₆-co-HEAA₂₅)-SC(=S)SC₂H₅ (A4) as Macro-CTA and ACPA as an initiator.

Relationship of molecular weight to particle size and morphology. By examining the hydrodynamic volume of nanoparticles made from the macro-CTA A3 (excepting Rxn 3 in Table 3), a linear relationship between molecular weight of diblock copolymer and the nanoparticle volume was evident. Importantly, the particle size not only increased with conversion but also with molecular weight (Figure 4). These linear relationships provide a useful handle for generating functional and uniform polymer nanoparticles with controllable particle sizes for many potential applications. For instance, such particles may be useful in surface coatings, rapid DNA sequencing, *in vitro* diagnosis exploiting antibody-antigen interactions, etc.⁵⁴⁻⁵⁶ In addition, the nearly complete conversion (i.e., low residual styrene in the latex) and the potential for surface-functionalization of the resulting nanoparticles are significant advantages for biomedical applications.^{57,58} The linear relationship between particle size and molecular weight might stem from the aforementioned one-to-one copy characteristics (i.e., or ideal miniemulsion) of this emulsion system. Because the N_c and N_{MCTA} are unchanged during the polymerization, the particle size may be directly related to the molar feed ratio of monomer and macro-CTA, which also determines the final molecular weight. However, the linear relationship between particle size and molecular weight in this system does not follow the packing parameter theory, which is often used to explain morphology transformations during emulsion or aqueous dispersion polymerization.^{59,60} The packing parameter theory proposes that during growth of the hydrophobic cores, the volume of these cores increases, causing changes of particle morphology from sphere to worm and then to vesicle to maintain the optimal surface energy of the particles.^{61,62} When using A3 and A4 as macro-stabilizers, no change in morphology was observed even when the hydrodynamic diameter of the core increased to 174 nm and the solids content (~ 20%) was in the range expected to facilitate morphology transformation (i.e., 10% to 25%).⁶³ One hypothesis for this observation may be that the chain lengths of the A3 and A4 macro-stabilizers are too long to trigger the transformation of morphologies.⁶⁴ To test this hypothesis, short macro-CTAs A1 and A2 with molecular weight in the appropriate range for formation of worm and vesicle morphology were synthesized (see Table 1).⁶⁵ MWDs in Figure S5 and SEC data in Table 3

for Reactions 5 and 6 again confirmed the excellent control over the synthesis of polystyrene diblock copolymer, even when very short macro-stabilizers were used. Surprisingly, TEM images in Figure 5 and DLS data in Table 3 showed that uniform spherical nanoparticles were consistently formed, even when the chain length of the polystyrene core was well above the threshold for the formation of worm and vesicle morphology.⁶⁵ These results imply that the packing parameter theory alone is not applicable for all PISA systems and hence novel or supplemental theoretical models are needed to fully understand the equilibrium morphology of soft nanoparticles. Based on the current data for the emulsion polymerization of styrene using P(PEGA-co-HEAA)-SC(=S)SC₂H₅ as the macro-stabilizer, it is possible to draw conclusions regarding the linear relationship of the diblock copolymer molecular weight with particle size, but not with particle morphology.

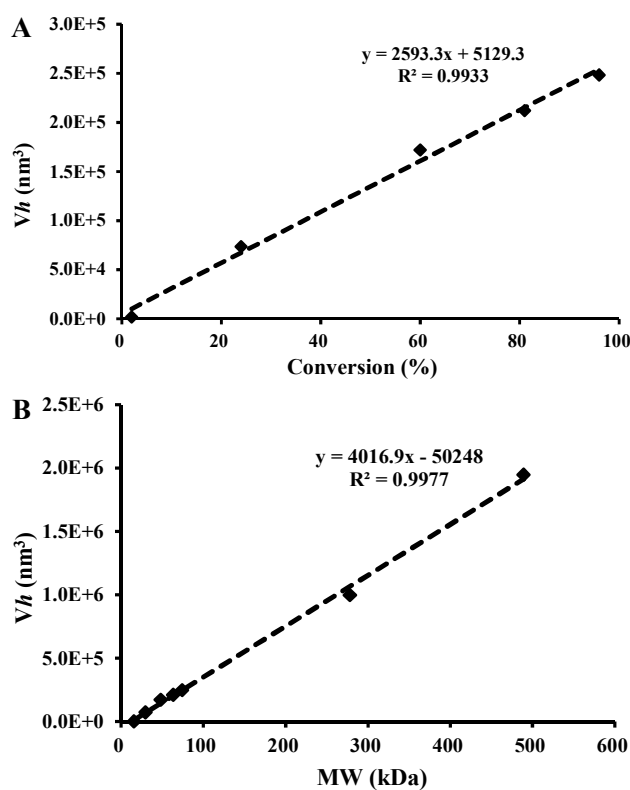


Figure 4. Linear relationship between (A) volume of particle (V_h) and Conversion, and (B) V_h and M_n for the RAFT-mediated emulsion polymerization of styrene in water at 80 °C using P(PEGA₂₁-co-HEAA₂₁)-SC(=S)SC₂H₅ (A3) as macro-CTA and ACPA as an initiator.

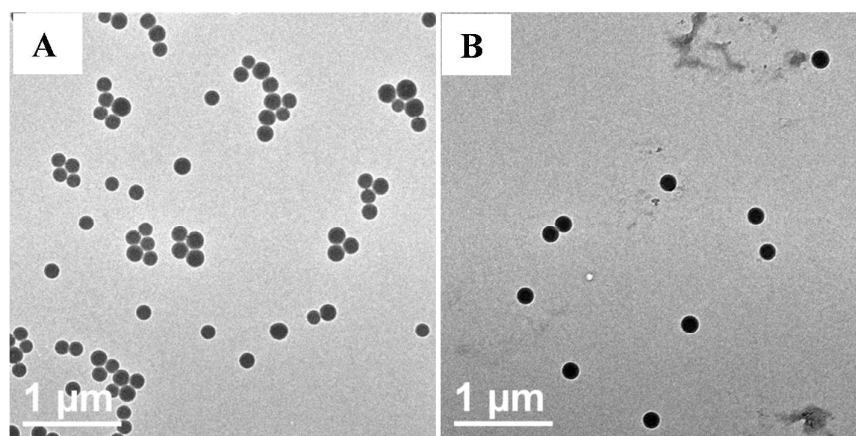


Figure 5. TEM images of the particles formed by RAFT-mediated emulsion polymerization of styrene in water at 80 °C for 6 h using ACPA as an initiator and (A) P(PEGA₁₅-co-HEAA₁₅)-SC(=S)SC₂H₅ (A2) and (B) P(PEGA₇-co-HEAA₇)-SC(=S)SC₂H₅ (A1) as macro-CTAs.

Conclusion

Ultrahigh molecular weight, well-defined polystyrene diblock copolymers were successfully synthesized for the first time by employing an emulsion polymerization technique using P(PEGA-co-HEAA)-SC(=S)SC₂H₅ as a dual macro-CTA / macrostabilizer. Our novel technique provided the following advantages: (i) ultrafast synthesis; (ii) minimal side reactions; (iii) ultrahigh molecular weight; (iv) little or no bimolecular coupling at nearly complete conversion; (v) narrow distribution of molecular weights and particle sizes; (vi) precise control over both molecular weight and particle size; (vii) no use of surfactants or organic solvents; (viii) high solids content; and (ix) excellent stability. The uniform nanoparticles formed, comprising styrenic cores and biocompatible shells, may find many novel applications in biomedical engineering in addition to traditional polymer industries.

Acknowledgements

This work was carried out within the Australian Research Council (ARC) Centre of Excellence in Convergent Bio-Nano Science and Technology (Project No. CE140100036). T.P.D. is grateful for the award of an Australian Laureate Fellowship from the ARC. N.P.T. acknowledges the financial support from Faculty of Pharmacy and Pharmaceutical Sciences, Monash University.

References

- (1) Cobo, I.; Li, M.; Sumerlin, B. S.; Perrier, S. *Nat. Mater.* **2014**.
- (2) Matyjaszewski, K.; Tsarevsky, N. V. *Nat. Chem.* **2009**, *1*, 276.
- (3) Jenkins, A. D.; Jones, R. G.; Moad, G. *Pure Appl. Chem.* **2010**, *82*, 483.
- (4) Matyjaszewski, K. *Macromolecules* **2012**, *45*, 4015.
- (5) Hawker, C. J.; Bosman, A. W.; Harth, E. *Chem. Rev.* **2001**, *101*, 3661.
- (6) Moad, G.; Rizzardo, E.; Thang, S. H. *Aust. J. Chem.* **2012**, *65*, 985.
- (7) Semsarilar, M.; Perrier, S. *Nat. Chem.* **2010**, *2*, 811.
- (8) Landfester, K. *Angew. Chem. Int. Edit.* **2009**, *48*, 4488.
- (9) Gody, G.; Maschmeyer, T.; Zetterlund, P. B.; Perrier, S. *Nat. Commun.* **2013**, *4*.
- (10) Read, E.; Guinaudeau, A.; Wilson, D. J.; Cadix, A.; Violleau, F.; Destarac, M. *Polym Chem-Uk* **2014**, *5*, 2202.
- (11) Percec, V.; Guliashvili, T.; Ladislaw, J. S.; Wistrand, A.; Stjern Dahl, A.; Sienkowska, M. J.; Monteiro, M. J.; Sahoo, S. *J. Am. Chem. Soc.* **2006**, *128*, 14156.
- (12) Simms, R. W.; Cunningham, M. F. *Macromolecules* **2007**, *40*, 860.
- (13) Nguyen, N. H.; Leng, X. F.; Percec, V. *Polym Chem-Uk* **2013**, *4*, 2760.
- (14) Mao, B. W.; Gan, L. H.; Gan, Y. Y. *Polymer* **2006**, *47*, 3017.
- (15) Rzyayev, J.; Penelle, J. *Angew. Chem. Int. Edit.* **2004**, *43*, 1691.
- (16) Holtze, C.; Antonietti, M.; Tauer, K. *Macromolecules* **2006**, *39*, 5720.
- (17) Correa, R.; Gonzalez, G.; Dougar, V. *Polymer* **1998**, *39*, 1471.
- (18) Jiang, L. M.; Shen, Z. Q.; Yang, Y. H.; Zhang, Y. F. *Polym. Int.* **2001**, *50*, 63.
- (19) Laurino, P.; Hernandez, H. F.; Brauer, J.; Kruger, K.; Grutzmacher, H.; Tauer, K.; Seeberger, P. H. *Macromol. Rapid Commun.* **2012**, *33*, 1770.
- (20) Kessel, S.; Truong, N. P.; Jia, Z. F.; Monteiro, M. J. *J. Polym. Sci., Part A: Polym. Chem.* **2012**, *50*, 4879.
- (21) Jin, C.; Liu, C.; Jiang, B.; Yin, Q. J. *E-Polymers* **2012**.
- (22) Zayas, H. A.; Truong, N. P.; Valade, D.; Jia, Z. F.; Monteiro, M. J. *Polym Chem-Uk* **2013**, *4*, 592.
- (23) Fitzwater, S.; Chang, H. R.; Parker, H. Y.; Westmoreland, D. G. *Macromolecules* **1999**, *32*, 3183.
- (24) Kukulj, D.; Davis, T. P.; Gilbert, R. G. *Macromolecules* **1998**, *31*, 994.
- (25) Odian, G. G. *Principles of polymerization*; 4th ed.; Wiley-Interscience: Hoboken, N.J., 2004.
- (26) Monteiro, M. J.; Cunningham, M. F. *Macromolecules* **2012**, *45*, 4939.
- (27) Zetterlund, P. B.; Kagawa, Y.; Okubo, M. *Chem. Rev.* **2008**, *108*, 3747.
- (28) Monteiro, M. J. *Macromolecules* **2010**, *43*, 1159.

- (29) Ho, K. M.; Li, W. Y.; Wong, C. H.; Li, P. *Colloid Polym. Sci.* **2010**, *288*, 1503.
- (30) El-Aasser, M. S.; Tang, J. S.; Wang, X. R.; Daniels, E. S.; Dimonie, V. L.; Sudol, E. D. *J Coating Technol* **2001**, *73*, 51.
- (31) Qiu, J.; Charleux, B.; Matyjaszewski, K. *Prog. Polym. Sci.* **2001**, *26*, 2083.
- (32) Jia, Z. F.; Truong, N. P.; Monteiro, M. J. *Polym Chem-Uk* **2013**, *4*, 233.
- (33) Pham, B. T. T.; Nguyen, D.; Ferguson, C. J.; Hawckett, B. S.; Serelis, A. K.; Such, C. H. *Macromolecules* **2003**, *36*, 8907.
- (34) Wang, X. G.; Luo, Y. W.; Li, B. G.; Zhu, S. P. *Macromolecules* **2009**, *42*, 6414.
- (35) Weber, W. G.; McLeary, J. B.; Sanderson, R. D. *Tetrahedron Lett.* **2006**, *47*, 4771.
- (36) Tao, L.; Liu, J. Q.; Davis, T. P. *Biomacromolecules* **2009**, *10*, 2847.
- (37) Tran, N. T. D.; Truong, N. P.; Gu, W. Y.; Jia, Z. F.; Cooper, M. A.; Monteiro, M. J. *Biomacromolecules* **2013**, *14*, 495.
- (38) Smith, A. E.; Xu, X. W.; McCormick, C. L. *Prog. Polym. Sci.* **2010**, *35*, 45.
- (39) Rieger, J.; Stoffelbach, F.; Bui, C.; Alaimo, D.; Jerome, C.; Charleux, B. *Macromolecules* **2008**, *41*, 4065.
- (40) Boursier, T.; Chaduc, I.; Rieger, J.; D'Agosto, F.; Lansalot, M.; Charleux, B. *Polym Chem-Uk* **2011**, *2*, 355.
- (41) dos Santos, A. M.; Le Bris, T.; Graillat, C.; D'Agosto, F.; Lansalot, M. *Macromolecules* **2009**, *42*, 946.
- (42) Zhao, C.; Patel, K.; Aichinger, L. M.; Liu, Z. Q.; Hu, R. D.; Chen, H.; Li, X. S.; Li, L. Y.; Zhang, G.; Chang, Y.; Zheng, J. *Rsc Adv* **2013**, *3*, 19991.
- (43) Qiao, Z. Y.; Du, F. S.; Zhang, R.; Liang, D. H.; Li, Z. C. *Macromolecules* **2010**, *43*, 6485.
- (44) Zhao, C.; Zheng, J. *Biomacromolecules* **2011**, *12*, 4071.
- (45) Oh, J. K.; Drumright, R.; Siegwart, D. J.; Matyjaszewski, K. *Prog. Polym. Sci.* **2008**, *33*, 448.
- (46) Smith, D.; Holley, A. C.; McCormick, C. L. *Polym Chem-Uk* **2011**, *2*, 1428.
- (47) Liang, M.; Lin, I. C.; Whittaker, M. R.; Minchin, R. F.; Monteiro, M. J.; Toth, I. *ACS Nano* **2010**, *4*, 403.
- (48) Zhao, W.; Gody, G.; Dong, S. M.; Zetterlund, P. B.; Perrier, S. *Polym Chem-Uk* **2014**, *5*, 6990.
- (49) Ferguson, C. J.; Hughes, R. J.; Pham, B. T. T.; Hawckett, B. S.; Gilbert, R. G.; Serelis, A. K.; Such, C. H. *Macromolecules* **2002**, *35*, 9243.
- (50) Chaduc, I.; Crepet, A.; Boyron, O.; Charleux, B.; D'Agosto, F.; Lansalot, M. *Macromolecules* **2013**, *46*, 6013.
- (51) Zetterlund, P. B.; Okubo, M. *Macromolecules* **2006**, *39*, 8959.
- (52) Yang, L.; Luo, Y. W.; Liu, X. Z.; Li, B. G. *Polymer* **2009**, *50*, 4334.
- (53) Ferguson, C. J.; Hughes, R. J.; Nguyen, D.; Pham, B. T. T.; Gilbert, R. G.; Serelis, A. K.; Such, C. H.; Hawckett, B. S. *Macromolecules* **2005**, *38*, 2191.
- (54) Rothberg, J. M.; Hinz, W.; Rearick, T. M.; Schultz, J.; Mileski, W.; Davey, M.; Leamon, J. H.; Johnson, K.; Milgrew, M. J.; Edwards, M.; Hoon, J.; Simons, J. F.; Marran, D.; Myers, J. W.; Davidson, J. F.; Branting, A.; Nobile, J. R.; Puc, B. P.; Light, D.; Clark, T. A.; Huber, M.; Branciforte, J. T.; Stoner, I. B.; Cawley, S. E.; Lyons, M.; Fu, Y. T.; Homer, N.; Sedova, M.; Miao, X.; Reed, B.; Sabina, J.; Feierstein, E.; Schorn, M.; Alanjary, M.; Dimalanta, E.; Dressman, D.; Kasinskas, R.; Sokolsky, T.; Fidanza, J. A.; Namsaraev, E.; McKernan, K. J.; Williams, A.; Roth, G. T.; Bustillo, J. *Nature* **2011**, *475*, 348.
- (55) Mahmoudi, M.; Lynch, I.; Ejtehadi, M. R.; Monopoli, M. P.; Bombelli, F. B.; Laurent, S. *Chem. Rev.* **2011**, *111*, 5610.
- (56) Hartono, S. B.; Phuoc, N. T.; Yu, M. H.; Jia, Z. F.; Monteiro, M. J.; Qiao, S. H.; Yu, C. Z. *J Mater Chem B* **2014**, *2*, 718.
- (57) Truong, N. P.; Whittaker, M. R.; Mak, C. W.; Davis, T. P. *Expert Opin. Drug Deliv.* **2015**, *12*, 129.

- (58) Jia, Z. F.; Bobrin, V. A.; Truong, N. P.; Gillard, M.; Monteiro, M. J. *J. Am. Chem. Soc.* **2014**, *136*, 5824.
- (59) Warren, N. J.; Armes, S. P. *J. Am. Chem. Soc.* **2014**, *136*, 10174.
- (60) Charleux, B.; Delaittre, G.; Rieger, J.; D'Agosto, F. *Macromolecules* **2012**, *45*, 6753.
- (61) Israelachvili, J. N.; Mitchell, D. J.; Ninham, B. W. *J. Chem. Soc., Faraday Trans. 2* **1976**, *72*, 1525.
- (62) Israelachvili, J. N. *Intermolecular and Surface Forces, 3rd Edition* **2011**, 1.
- (63) Sugihara, S.; Blanazs, A.; Armes, S. P.; Ryan, A. J.; Lewis, A. L. *J. Am. Chem. Soc.* **2011**, *133*, 15707.
- (64) Blanazs, A.; Ryan, A. J.; Armes, S. P. *Macromolecules* **2012**, *45*, 5099.
- (65) Zhang, X. W.; Boisse, S.; Zhang, W. J.; Beaunier, P.; D'Agosto, F.; Rieger, J.; Charleux, B. *Macromolecules* **2011**, *44*, 4149.